Applied Physics A (2021) 127:300
https://doi.org/10.1007/s00339-021-04438-4

Applied Physics A
Materials Science & Processing

Production and characterization of titanium oxide nanoparticle using extract of macrophytic alga

Syazwan Paraja[1] · Subash C. B. Gopinath[1,2] · Periasamy Anbu[3] · M. K. Md Arshad[1,4] · N. A. Parmin[1] · Iswary Letchumanan[1] · Chun Hong Voon[1] · Thangavel Lakshmipriya[1] · Nurshamira Shohaimi[1] · Ahmad Radi Wan Yaakub[2]

Received: 5 November 2019 / Accepted: 15 March 2021 / Published online: 1 April 2021

Abstract
This study described a "green chemistry" synthesis of titanium oxide nanoparticle (TiO_2-NP) using environment-friendly reducing agents that were from *Elodea canadensis*. The obtained TiO_2-NP has an intense surface plasmon reverberation band at ~ 250 nm with UV–visible spectroscopic investigation which showed the intactness of TiO_2-NPs. The morphological behaviour of TiO_2-NPs was watched beneath field-emission scanning electron microscopy and transmission electron microscopy, shown that TiO_2-NPs have a spherical pattern with a normal estimate of ~ 25 nm in breadth. The occurrence of the critical elements was pinpointed by energy-dispersive X-ray spectroscopy study, which displays the predominant titanium and oxide elements. Further support with a defined morphology and size distribution was rendered by atomic force microscopy and 3D high-power microscopy analyses. X-ray powder diffraction and chosen area electron diffraction examinations affirmed that TiO_2-NPs are crystal clear in macrocosm. X-ray photoelectron spectroscopy study was uncovered natural composition of the TiO_2-NPs, displaying Ti 2*p* crested at 458.48 eV with C1*s* crest for the catalyst that was shaped into a C–H constitute at 284.88 eV. The O 1*s* spectra moreover were displayed with authoritative vitality at 532.28 eV. XRD analysis gave proportion phase as 75%:25% for anatase and rutile. DLS showed polydispersity index esteem of − 1.23, and zeta potential for green synthesized Ti_2O-NPs was − 3.87 mV. A broad hydroxyl peak was identified, and prominent peaks were notified at 1631.78 cm^{-1} and 3454.51 cm^{-1} by Fourier-transform infrared spectroscopy analysis.

Keywords Titanium oxide nanoparticle · *Elodea canadensis* · Macrophyte · Green synthesis

1 Introduction

The dominion of nanotechnology basically encompasses with science, material science, chemistry and fabric sciences, and it creates off-beat helpful nanosized materials for biomedical and prophylactic practices [1–3]. The organic blends of nanoparticles are being executed by diverse macro–microscopic living beings such as weed, microscopic organisms, parasites, ocean growth and microalgae [4]. The biocreated nanomaterials have been viably governing different endemic illnesses with nether antagonistic impact. The weed comprehends copious characteristic composites such as flavonoids, alkaloids, saponins, tannins, steroids and other wholesome mixtures. These are determined from different districts of the weed such as clears out, roots, stems, shoots, blooms, seeds and barks. As of late, numerous considers have been demonstrated that the weed extricates act as a capable antecedent for the amalgamation of nanomaterial in

✉ Subash C. B. Gopinath
subash@unimap.edu.my

✉ Periasamy Anbu
anbu25@inha.ac.kr

[1] Institute of Nano Electronic Engineering, Universiti Malaysia Perlis, 01000 Kangar, Perlis, Malaysia

[2] Faculty of Chemical Engineering Technology, Universiti Malaysia Perlis, 02600 Arau, Perlis, Malaysia

[3] Department of Biological Engineering, College of Engineering, Inha University, Incheon 402-751, Republic of Korea

[4] Faculty of Electronic Engineering Technology, Universiti Malaysia Perlis, 02600 Pauh, Perlis, Malaysia

non-venturesome policies. Inasmuch as the plant extricates comprise different auxiliary metabolites, they act as decreasing and stiffening operators for the biolessening response to the amalgamated novel metallic nanoparticles [5–9]. The non-biological strategies (physical and chemical) are used within the amalgamation of nanoparticles that contains a genuine perilous and tall harmfulness for living beings. In the expansion, the organic amalgamation of metallic nanoparticles is reasonable, unattached step and environmentally strategies. The weeds are effectively utilized within the blend of different greener nanoparticles such as cobalt, magnetite, platinum, titanium, gold, copper, palladium, silver and zinc oxide [4, 8, 10]. Moreover, the plant adjudicated nanoparticles are a potential cure for miscellaneous maladies such as HIV, intestinal sickness, hepatitis, cancer and other intense illnesses [11].

Currently, the titanium oxide nanoparticle (TiO_2-NP) has several applications including photocatalytic, photoconductivity, reducing toxicity of dyes and pharmaceutical drugs and reproduction of silkworm [6, 12–15]. In addition, the TiO_2-NP was also used to decompose the organic compounds in wastewater [16]. To enhance the potentials of the TiO_2-NP, in the present study we have desired the macrophyte/halophyte for the efficient production of TiO_2-NP by the bioreduction reaction. We desired to use the algal species *Elodea c*anadensis and extracted the compounds reside. The obtained TiO_2-NP was confirmed with the morphological characterizations by availing atomic force microscopy, scanning electron microscopy, transmission electron microscopy and 3D high-power microscopy analyses. Further, chemical and structural characterizations were done by X-ray photoelectron spectroscopy, energy-dispersive X-ray powder diffraction, X-ray spectroscopy and Fourier-transform infrared spectroscopy studies. The stability and the cumulative size were defined by dynamic light scattering.

2 Materials and methods

The weed species *Elodea canadensis* was accumulated from the area at Kuala Perlis, Perlis Malaysia. Titanium(IV) oxide and filter membranes were bought from SIGMA-ALDRICH (USA) and Hitotsu (Japan), respectively. pH indicator strips (non-bleeding) were purchased from MColorpHast, Germany. The rest of the reagents applied were of analytical classification, and all other reagents were kept as sanctioned by the constructor.

2.1 Extraction of *E. canadensis* compounds

The kelp was gathered and washed two times by plenty of water and one time by refined water to evacuate the waste materials that found at first glance. 0.025 g of the kelp that has been washed is arranged and cut into smaller pieces. The finely cut pieces at that point were blended with the refined water and smashed. The ocean growth is overflowed with 50 ml of refined water for around 15 min at that point permitted to chill off to the room temperature. The ocean growth separate is gathered by the filtration using filter film (0.45 µm) which eventually stored at 4 °C for further process to act as reducing and cloaking agent [7, 17].

2.2 Production of TiO_2-NPs

Previous to *E. canadensis* extract preparation, it was continued by using 20 ml of stored kelp separate. They were added dropwise to the prepared 100 mg of titanium tetra oxide with 80 ml of distilled water and blended for a whole night at the room temperature. Subsequent to mixing the samples were pipetted and were stirred for around 15 min to gather the pellets and removed the supernatants for purification purpose. The purification then was repeated by stirring using distilled water two times. Finally, the obtained pellets as the nanoparticles were stored at 4 °C.

2.3 Studies on TiO_2-NPs

The production of TiO_2-NPs was affirmed using UV–Vis spectrophotometry explication (UV–Vis nanodrop), scanned at 250–750 nm. The highest peak of the retention within the UV range ought to show the highest TiO_2-NPs amount within the response blend (the most elevated surrender). Field-emission scanning electron microscopy (FE-SEM; Hitachi, S-4300SE, Japan) was exploited to determine the size and morphology, whereas the elemental compositions involving titanium from the samples were identified by energy-dispersive X-ray (EDX; EDAX, USA). A JEM 2100F microscope (Japan) was used to perform field emission-transmission electron microscopy (FE-TEM). Initially, the preparation of samples was done by fixing a drop of TiO_2-NPs suspension on a carbon-covered copper grid, and at that point, the morsels were dried exploiting a vacuum desiccator. There were various magnifications used to get the nanoparticles images. An atomic force microscope (Nano-Scope, Ica, Vecco, USA) was also used to analyse the shape and size of the TiO_2-NPs. AFM was used to determine the morphology by placing the TiO_2-NPs samples on a silicon wafer followed by AFM scanning.

X-ray powder diffraction that used a DMAX-2500 (Rigaku, Japan) was applied to analyse the synthesized TiO_2-NPs. XRD system was embedded with a Cu Kα (1.54059 Å) radiation fountainhead and a nickel filter. There were various diffraction angles set-up around 10°–90° range and the appending occurrence was 0.5/s. In order to analyse the elemental and chemical structure at the first glance of TiO_2-NPs, X-ray photoelectron spectroscopy (XPS; Thermo

Scientific, K-Alpha, UK) was applied. Dynamic light scattering (DLS) that used an ELS-Z particle size examiner and the zeta potential (Photal Otsuka Electronics, Japan) was applied in order to get the size distribution and solidity of TiO_2-NPs. Fourier-transform infrared (FTIR) spectroscopy was carried out to clarify the molecular mould of TiO_2-NPs. This explication to chronicle the infrared spectrum of TiO_2-NPs by either rumination or promulgation of a sample was handled using a Vertex 80 V FTIR system (Bruker, Germany). A build-up of KBr pellet with TiO_2-NPs was required for another site of aim to interpret the FTIR spectrum from 4000 to 400 cm^{-1}.

3 Results and discussion

The macrophyte *E. canadensis* contains plentiful normal constituents like saponins, alkaloids, tannins, steroids, flavonoids and other dietary mixes. These regular modules are obtained from different portions of the plant, for example, blossoms, leaves, roots, stems, seeds, shoots and barks. As of late, numerous investigations have been demonstrated that the plant separates go about as an inherent antecedent for the combination of nanomaterial in non-unsafe ways [5, 7, 8, 11]. Inasmuch as the plant extract exhibits different auxiliary metabolites, it goes about as diminishing and balancing out specialists for the biolessening response to orchestrate the off-beat metallic nanoparticles. The non-natural techniques (concoction and physical) were utilized in the combination of nanoparticles that has a genuinely dangerous and consequential harmfulness for living forms. Moreover, the organic union of metallic nanoparticles is modest, single-step and eco-accommodating strategies [18]. Therefore, the present examination was directed to the synthesis of titanium nanoparticle (TiO_2-NP) utilizing *E. canadensis* and affirmed by morphological and structural characterizations.

3.1 Synthesis of TiO_2-NPs and preliminary analysis

Initially, to produce TiO_2-NPs different volumes of algae extracts (10 ml and 20 ml) with a constant amount of TiO_4 was added as 100 mg and resulting 20 ml solution was the best for making TiO_2-NPs. Comparing between 10 and 20 ml is actually to avoid from error due to the high optical density of the solution by diluting them to 1:4 with the distilled water. From 10 ml, the cloudy colour was changed to more clear at 20 ml. After mixing the plant extracts and TiO_4, the colour was changed which could verify the formation of TiO_2-NPs in the suspension (Fig. 1). This sample was then analysed under UV–Vis spectrum using nanodrop at 250–750 nm, and the pH of the sample was found to be 5.5 which is placed among optimal pH range (3.2–6.8) for TiO_2-NPs.

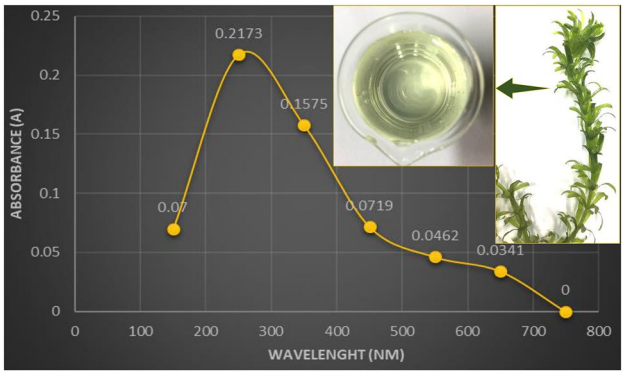

Fig. 1 UV–Vis spectrum by nanodrop showing the formation of TiO_2-NPs. Insets show a photograph of *E. canadensis*

3.2 Characterizations of TiO_2-NPs

3.2.1 UV–Vis spectroscopy

UV–visible spectroscopy is a basic draw near to optically analyse assembled TiO_2-NPs. The union of TiO_2-NPs was affirmed by the situating of the first glance plasmon reverberation in the UV–Vis spectroscopic investigation. The surface plasmon response (SPR) spectra of the blend of *E. canadensis* bark extract-wrapped TiO_2-NPs were proving as a peak discovered at ~ 250 nm (Fig. 1). The crest within the UV spectrum was added owing to the impacts of SPR of electrons within the TiO_2-NPs arrangement [19]. The crest shape within the UV–visible spectrum is impacted by the measure, morphology and shape of the TiO_2-NPs being aggregated. A few consider having demonstrated that the visible area of TiO_2-NPs absorbance by UV–visible spectroscopy is 250–750 nm. The wide extent of the assimilation band coincides to different shapes and sizes of TiO_2-NPs. The round formed TiO_2NPs up holds to the assimilation band at 250–750 nm in the UV–visible range [20]. The washing and centrifugation of TiO_2-NPs eliminated the debasements within the frame of the supernatant. The pellet, while re-dissipated in water, appeared well-defined SPR at 250 nm.

3.2.2 Transmission electron microscopy (TEM)

The size and shape of *E. canadensis* extract-wrapped TiO_2-NPs were investigated utilizing the TEM. Figure 2a, b shows the picture of biologically aggregated TiO_2-NPs, where the grid borders of a nanoparticle are displayed accurately. Figure 2a shows a conscripted courtyard electron diffraction (SAED) design of the assembled particles. The one shinning spots within the picture clearly show that the TiO_2-NPs are crystal clear in macrocosm. The

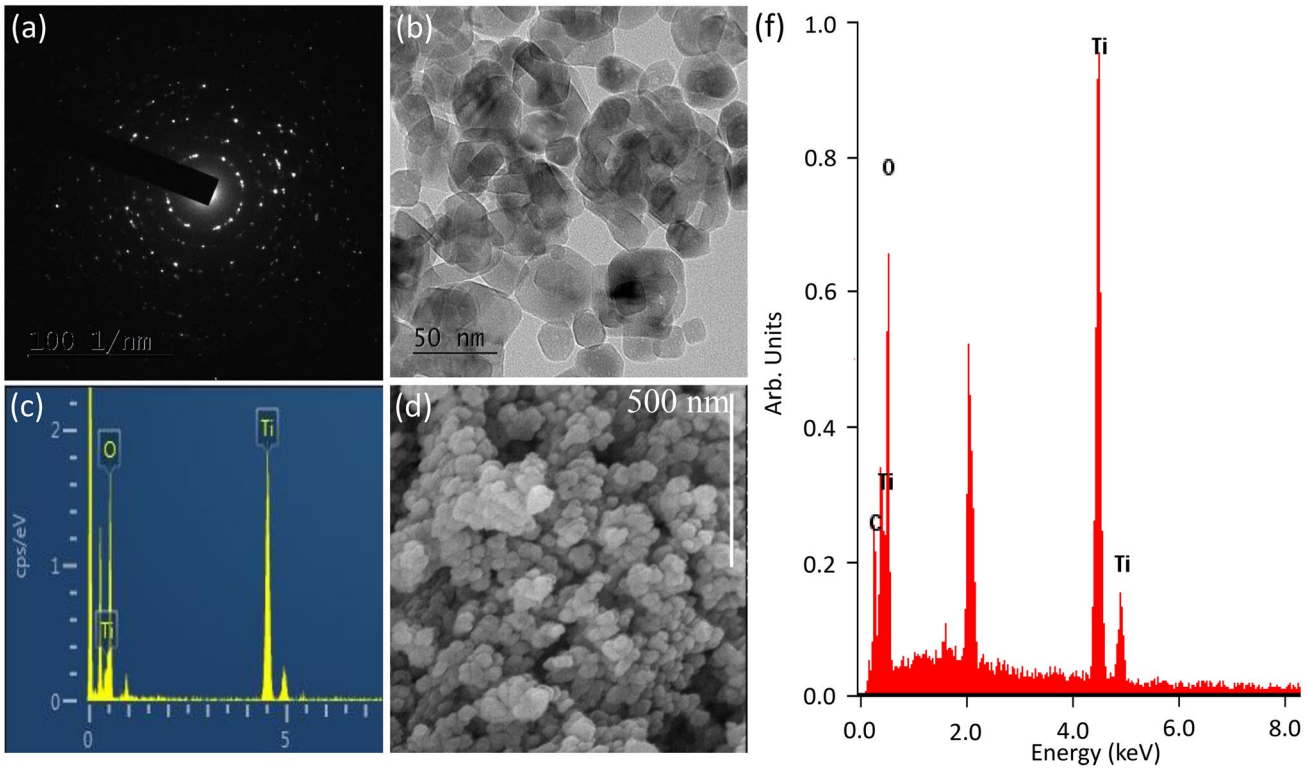

Fig. 2 Morphological features of eco-friendly synthesized TiO_2-NPs. **a** SAED analysis of TiO_2-NPs by TEM; **b** TEM image at 50 nm scale; **c** EDX analysis by TEM; **d** FESEM showing the images of TiO_2-NPs at 500 nm; **e** EDX analysis by FESEM

TEM picture uncovers that the TiO_2-NPs produced were roundly shaped particles with smooth outsides. The figures at diverse amplification of TEM showed that nearly each of the TiO_2-NPs synthesized had comparable ranges of sizes and about round shape. TEM pictures recommended that the assembled TiO_2-NPs were thoroughly scattered without totals of the nanoparticles. The sizes of the TiO_2-NPs were found to be extended between 10 and 50 nm with a normal measure of ~ 25 nm (Fig. 2b). There were many forms of TiO_2-NPs clusters within the image, which are anticipated to impact the variety in molecule estimate of TiO_2-NPs. The calculation of the TiO_2-NPs was estimated in corresponding with the measure watched within the TEM pictures. Figure 2c shows the EDX inquiry (after TEM) of organically synthesized TiO_2-NPs utilizing the *E. canadensis* bark extricates. EDX investigation uncovered the quantitative status of the components which will be included within the arrangement of TiO_2-NPs. It is utilized to decide the sum of each component present in TiO_2-NPs [21]. The top escalate is corresponding to the sum of TiO_2-NPs synthesized. The stack of TiO_2-NPs shape is subordinate on the amount of TiO_2 displayed within the solution. The crest raised at 2 keV is due to TiO_2 and affirms the arrangement of the reduced TiO_2-NPs.

3.2.3 Field-emission scanning electron microscope (FESEM)

FESEM investigation was too connected to assess the shape of the nanoparticles synthesized. Figure 2d shows a high-density image of TiO_2-NPs which was aggregated utilizing the *E. canadensis* bark extricate suspension. The pictures precisely delineate the moderately circular and comparable shape of the amalgamated TiO_2-NPs. Based on FESEM pictures, the estimate of the assembled TiO_2-NPs was betwixt 50 and 100 nm in breadth: it is bigger than the measure decided by TEM. The bigger measure of TiO_2-NPs has been enough to merit the conglomeration of TiO_2-NPs and the estimation of clustered TiO_2-NPs by FESEM [22]. Figure 2e shows a FESEM basic profile of TiO_2-NPs organically assembled implies the *E. canadensis* bark extricates arrangement. The spectral lines expanded at around 0.4, 4.5 and 5 keV for Ti and 0.5 keV for O eventually proved the presence of TiO_2-NPs. The unearthly line of C watched at 0.3 keV may emerge due to the catalyst constitute.

3.2.4 High-power microscopy and AFM analysis

The above analysis was further supported by the high-power microscopy with the 3D profile. Based on the obtained images, it was apparent that there are intact particles upon

synthesis (Fig. 3a). AFM was utilized for the particular inquisition of morphology and surface harshness of naturally synthesized TiO_2-NPs. The measure of size with TiO_2-NPs based on AFM examination was ~ 25 nm in distance across. This implies that the measure of TiO_2-NPs is near to the estimate of particles assessed by TEM and FESEM studies. The determination of AFM uncovered clustered TiO_2-NPs in which the distinct TiO_2-NPs shows up as a little blot of spherical shape. Not at all like TEM and SEM, AFM has given a legitimate and exact estimation of the tallness of a nanoparticle. From Fig. 3b, the tallness of amalgamated TiO_2-NPs is ~ 25 nm for a shrill and the rough conclusion of the molecule.

3.2.5 X-ray photoelectron spectroscopy (XPS)

E. canadensis extract-capped TiO_2-NPs were analysed by XPS to distinguish the changes in chemical oxidation states and surface proportion of TiO_2-NPs. The study looks of TiO_2-NPs showed that C 1*s*, O 1*s*, Ti 2*p* and Si 2*p* of the spectra had authoritative energies of 4377.68, 532.28, 10,769.3 and 99.18 eV individually (Fig. 4a–e). Enticingly, the titanium and oxygen had conspicuous crests and the carbon and silicon appeared to be the slighter indications from the outer region of the nanoparticles within the survey check. The C1*s* crest of the catalysts was shaped into a constituent C–H (4377.68 eV) (Fig. 4a). Based on Fig. 4b, the crest for O1*s* was watched at 532.28 eV. The top demonstrates the occupancy of carbonyl bunches on the surface of TiO_2-NPs [23]. Aside from 532.28 eV, there was another crest watched within the O1*s* check, which compares to the appearance of carbonates or metallic oxides on the first glance of TiO_2-NPs. This actually indicates the nearness of titanium on the TiO_2 NPs surface was more conspicuous which directly proved the examination of EDX by TEM and FESEM showed the powering titanium component on the TiO_2-NPs synthesized. Figure 4d shows the presence of elemental Si2*p* at 99.18 eV. The present apparent range is the C1*s* filter, and Fig. 4a shows the crest for the C1*s* filter watched at 4377.68 eV. TiO_2-NPs which have been uncovered to the air will show a perceptible amount of accidental carbon defilement ordinarily with a layer depth of 1–2 nm. The crest at 4377.68 eV was compared to the C–C constituent, by default. By the by, it is conceivable to get C–O e–C and O–C=O constituents on carbon-adulterated TiO_2-NPs [24].

3.2.6 X-ray powder diffraction (XRD)

Figure 5 shows XRD designs of *E. canadensis* extract-capped TiO_2-NPs. Based on the comparison with the titanium standard (JCPDS 04-0836), the Debye–Scherrer equation was utilized to decide normal crystallite breadth from the half thickness of the diffraction crests [25]. Five fundamental diffraction crests for TiO_2-NPs were watched at 2*q*¼ 27.81, 32.19, 46.17, 51.59 and 56.11, which is compared to the planes of face-centred cubic (fcc) TiO_2 gems at 75.06, 103.35, 55.64, 46.14 and 39.93, separately. Based

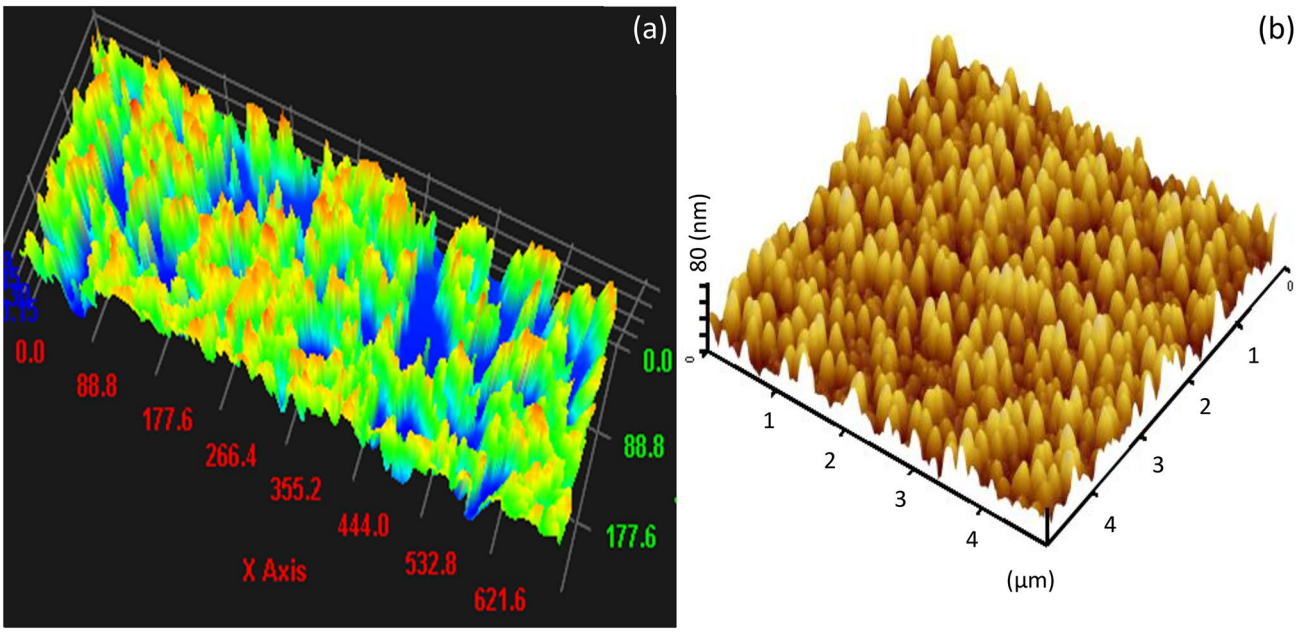

Fig. 3 Morphological observation. **a** 3D images of after TiO_2-NPs attachment on the silica wafer; **b** AFM images of synthesized TiO_2-NPs. The three-dimensional image is displayed

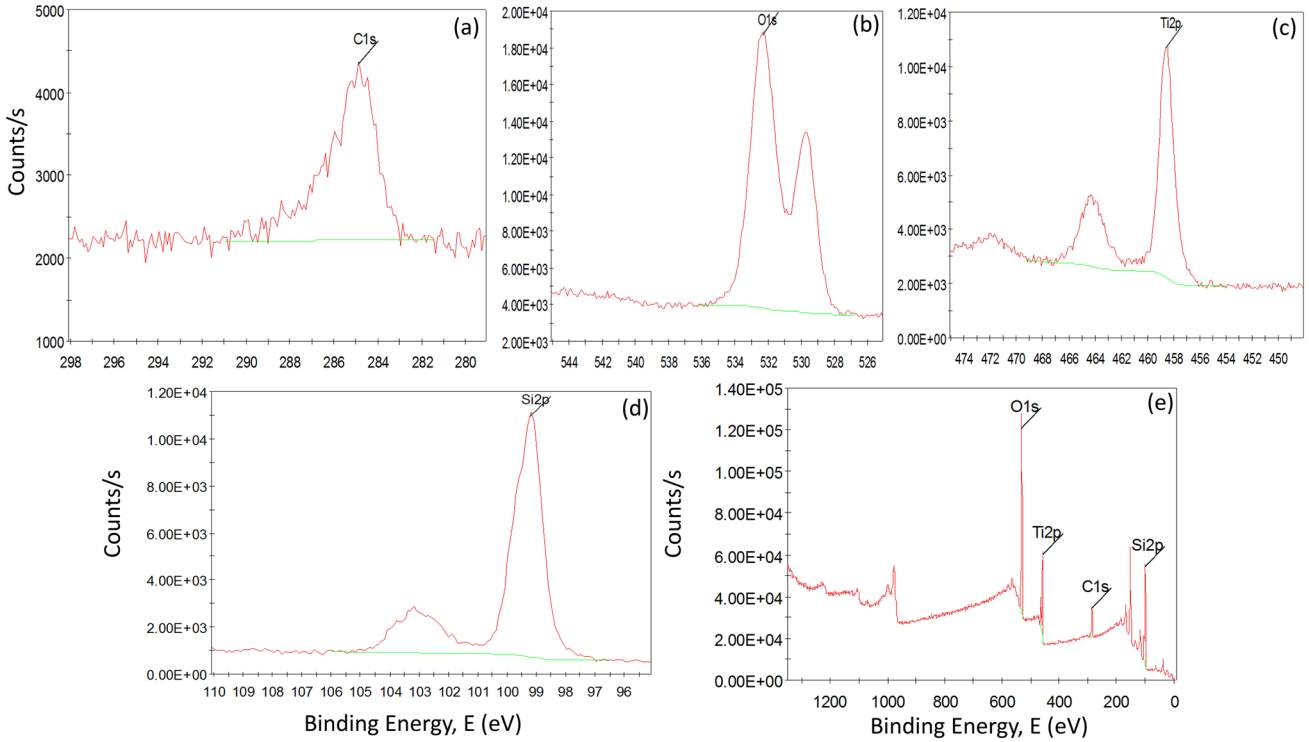

Fig. 4 XPS data for eco-friendly synthesized TiO_2-NPs. **a** C1*s* data; **b** oxygen O1*s* data; **c** Ti 2*p*; **d** silicon Si2*p* data; and **e** survey scan

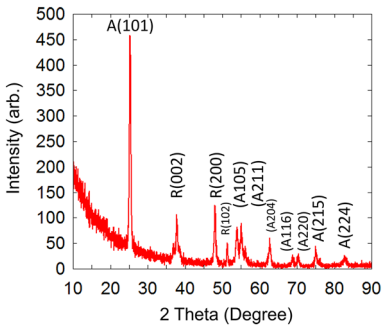

Fig. 5 XRD pattern of TiO_2-NPs synthesized using *E. canadensis* extract

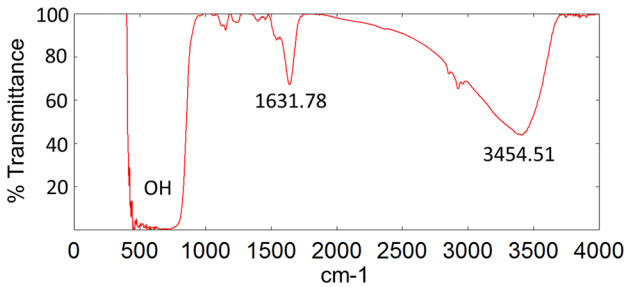

Fig. 6 FTIR spectrum of TiO_2-NPs synthesized using *E. canadensis* extract. The major peaks are indicated

on Fig. 5, all of the crests on this design have a place to anatase and rutile stages of these compounds. These crests have been checked as (*R*) for the rutile phase and (*A*) for the anatase phase individually on the diffraction design. The general composition phase between these two compounds has been known as 25% for rutile and 75% for anatase. The analysis in Fig. 5 provides this proportion as 25%:75% for rutile stage and anatase stage on the premise of greatest peak strength proportions for the particular both stages. No evidence of other TiO_2 stages including Zr- or brookite-based srilankite was watched which frequently show up in nearly of the nanocrystalline TiO_2 powders arranged by different pathways. The molecule measure within the rutile stage was recorded to be bigger compared to anatase by distinctive union forms since the agglomeration steps are the development of essential TiO_2 particles with an augmentation of warm vitality. The finding is in agreement with the prior X-ray and synchrotron X-ray diffraction information.

3.2.7 Fourier-transform infrared spectroscopy (FTIR)

FTIR spectra give adequate data on the biomolecule's existent in TiO_2-NPs. In this control, the spectra created by FTIR were recorded to distinguish the natural composites displayed on the nanoparticles that may be dependable for the lessening of TiO_4 to TiO_2 NPs as well as for wrapping the bioreduced TiO_2-NPs. In Fig. 6, the FTIR

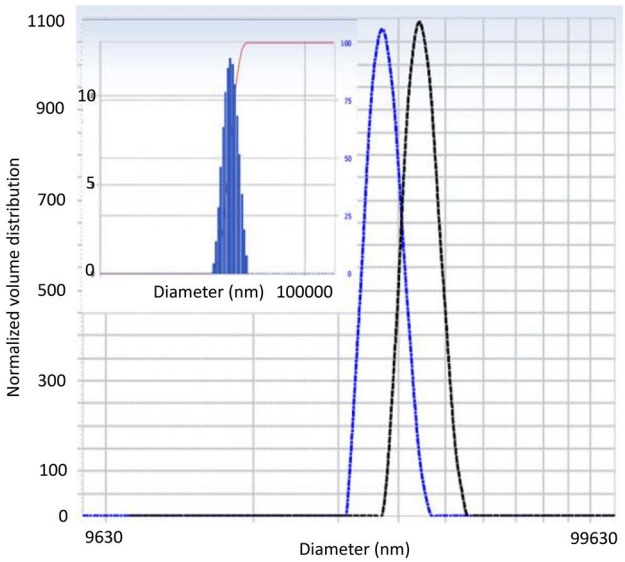

Fig. 7 Molecular estimate of the green synthesized TiO_2-NPs beneath DSL studies. Figure inset is the escalated dispersion of distance across for TiO_2-NPs

spectra produced for TiO_2-NPs are presented. Based on this analysis, the prominent peaks were notified at 1631.78 and 3454.51 cm^{-1} and the appearance of a broad hydroxyl peak was identified. The absorption band at 1631.78 is affiliated to bending and 3454.51 cm^{-1} to stretching vibration of O–H. These changes might have started from the bioreduction preparation.

3.2.8 Dynamic light scattering (DLS)

The molecule estimate of synthesized TiO_2-NPs was analysed by DLS. Refer to Fig. 7, the estimate of synthesized TiO_2-NPs is 61,455.0 nm in distance across. Molecule estimate dissemination showed the nearness of TiO_2-NPs with polydispersity file (PDI) esteem of − 1.29. The PDI value shows the extend nanoparticle measure dissemination. A higher reading of PDI reflects a more extensive extent of particles, while a lower reading of PDI reflects tests with equitably measured particles. The lower of PDI got for synthesized TiO_2-NPs shows that monodispersed TiO_2-NPs have more prominent molecule soundness. In addition, the solidness of nanoparticle is properly clarified by the estimation of the greatness of electrostatic charge fascination or repugnance betwixt the particles within the fluid environment. The estimation is communicated as zeta potential. Particles with zeta possibilities are in between + 30 and − 30 mV and are the characteristic of steady TiO_2-NPs. The zeta potential got for green production of TiO_2-NPs in this research (− 3.87 mV) shows that the TiO_2-NPs were steady, which have been evidenced by limit measure dissemination list.

4 Conclusion

In this research, the titanium dioxide nanoparticles were synthesized using *E. canadensis* by means of biological eco-friendly synthesis. Moreover, the characteristics of morphology affirmed the size (20–25 nm) and spherical shape of Ti_2O-NPs. In addition, XRD results of Ti_2O-NPs exhibited first two 2θ values at $R(002)$ and $A(101)$ that proved the theoretical proportion phase as 25%:75% and XPS result uncovered Ti_2O-NPs O1*s* peak at the top. FTIR result confirmed the presence of plant extracted components on Ti_2O-NPs. Altogether, these outcome confirmed the reduction of Ti_4O into Ti_2O-NPs. In general, the blend of Ti_2O-NPs utilizing plant extricate is basic, quick, cost-effective and naturally secure relative to chemical and physical strategies and the bioamalgamated Ti_2O-NPs have the prospects for utilizing different applications, especially within the area of biomedicine.

References

1. K.H. Suk, S.C.B. Gopinath, P. Anbu, T. Lakshmipriya, Powder Technol. **328**, 140 (2018)
2. S. Anniebell, S.C.B. Gopinath, Curr. Med. Chem. **25**, 1 (2018)
3. K.H. Suk, S.C.B. Gopinath, Curr. Med. Chem. **24**, 3310 (2017)
4. P. Kuppusamy, M.M. Yusoff, G.P. Maniam, N. Govindan, Saudi Pharm. J. **24**, 473 (2016)
5. S. Ramanathan, S.C.B. Gopinath, Microsyst. Technol. **23**, 1 (2017)
6. B. Ranjani, J. Kalaiyarasi, L. Pavithra, T. Devasena, K. Pandian, S.C.B. Gopinath, Microchim. Acta **185**, 194 (2018)
7. P. Anbu, S.C.B. Gopinath, H.S. Yun, C.-G. Lee, J. Mol. Struct. **1177**, 302 (2019)
8. J.R. Anasdass, P. Kannaiyan, R. Raghavachary, S.C.B. Gopinath, Y. Chen, PLoS ONE **13**, 1 (2018)
9. K.S. Radad, M.M. Al-Shraim, M.F. Moustafa, W.D. Rausch, Neurosciences **20**, 10 (2015)
10. P. Kuppusamy, M.M. Yusoff, N. Govindan, Saudi Pharm. J. **24**, 473 (2014)
11. M.E. Foo, P. Anbu, S.C.B. Gopinath, T. Lakshmipriya, C.-G. Lee, H.S. Yun, M.N.A. Uda, A.R.W. Yaakub, Surf. Interface Anal. **50**, 354 (2018)
12. Z. Schnepp, S.C. Wimbush, S. Mann, S.R. Hall, CrystEngComm **12**, 1410 (2010)
13. K. Lv, J. Yu, L. Cui, S. Chen, M. Li, J. Alloys Compd. **509**, 4557 (2011)
14. S. Dutta, A.K. Patra, S. De, A. Bhaumik, B. Saha, ACS Appl. Mater. Interfaces **4**, 1560 (2012)
15. M.B. Sogo, M. Serra, A. Primo, M. Alvaro, H. Garcia, ChemCatChem **5**, 513 (2013)
16. E. Sutisna, M. Wibowo, D.Y. Rokhmat, R. Rahman, M. Khairurrijal, M. Abdullah, Procedia Eng. **170**, 78 (2017)
17. S. Ramanathan, S.C.B. Gopinath, P. Anbu, T. Lakshmipriya, F.H. Kasim, C.G. Lee, J. Mol. Struct. **1160**, 80 (2018)

18. L. Contreras-Porcia, C. Lpez-Cristoffanini, in *Gel Electrophoresis: Advanced Techniques*, chap. 2. ed. by S. Magdeldin (InTech, Croatia, 2012), pp 21–50
19. Y. Lu, W. Dong, Z. Chen, A. Pors, Z. Wang, S.I. Bozhevolnyi, Sci. Rep. **6**, 1–9 (2016)
20. N.M. Abd-Alghafour, N.M. Ahmed, Z. Hassan, S.M. Mohammad, M. Bououdina, M.K.M. Ali, Nanosci. Nanotechnol. Lett. **8**, 181–186 (2016)
21. N. Marmiroli, J.C. White, Front. Plant Sci. **7**, 1370 (2016)
22. N. Poudyal, J.P. Liu, J. Wang, A.K. Mishra, Q. Zhao, L. Huang, J. Phys. D Appl. Phys. **46**, 043001 (2013)
23. S. Mehl, A. Toghan, T. Bauer, O. Brummel, N. Taccardi, P. Wasserscheid, J. Libuda, Langmuir **31**, 12126–12139 (2015)
24. S. Yu, H.J. Yun, Y.H. Kim, J. Yi, Appl. Catal. B Environ. **144**, 893–899 (2014)
25. S. Rani, P. Suri, P.K. Shishodia, R.M. Mehra, Sol. Energy Mater. Sol. Cells **92**, 1639 (2008)